The Stronger the Better: Donor Substituents Push Catalytic Activity of Molecular Chromium Olefin Polymerization Catalysts

Helge-Boj Hansen,[a] Hubert Wadepohl,[a] and Markus Enders*[a]

Abstract: The donor strength of bifunctional pyridine-cyclopentadienyl ligands was altered systematically by the introduction of donating groups in the *para*-position of the pyridine. In the resulting chromium complexes an almost linear correlation between donor strength and the nitrogen-chromium distance as well as the electronic absorption maximum is experimentally observed. The connection of electron-donating groups in the ligand backbone leads to an efficient transfer of the electronic influences to the catalytically active metal centre without restricting it through steric effects. Therefore, catalytic olefin polymerization activity, which is already very high for the previously studied catalysts, increase considerably by attaching *para*-amino groups to the chelating pyridine or quinoline, respectively. Combining electron-rich indenyl ligands with *para*-amino substituted pyridines lead to the highest catalytic activities observed so far for this class of organo chromium olefin polymerisation catalysts. The resulting polymers are of ultra-high molecular weight and the ability of the catalysts to incorporate co-monomers is also very high.

Introduction

Donor functionalized cyclopentadienyl (cp) based chromium complexes such as compounds **A**–**D** (Figure 1) are good pre-catalysts for ethylene polymerization.[1–5] The best catalyst properties in this series have so far been obtained by use of aromatic donor groups where the N-donor is separated by the five membered ring by a C_2 spacer (e.g. compounds **C** or **D**). Such systems are able to produce ultra-high molecular weight polyethylene (UHMWPE) with complex **C** being used in multi component catalyst systems that are able to produce PE blends with high UHMWPE content.[6–9]

The catalytic properties depend on the ligand structure and the electronic environment they offer to the metal centre. The donor strength of the chelating ligand can be altered by introduction of electron rich substituents at the N-donor (e.g. **B**) or at the five membered ring (e.g. alkyl groups in compounds **A**, **C** and **D** respectively). Previous studies showed that electron rich cyclopentadienyl or indenyl ligands improve catalytic activity and the ability to incorporate α-olefins such as 1-hexene to the polymer chain.[1–2,5,10] Therefore, we aimed to study the effect of the electron-donating ability of the neutral N-donor ligand on the catalytic properties in a systematic way (Figure 2).

It is well known that the basicity of aromatic donors such as pyridine has an influence on its coordination behaviour, the metal-nitrogen bond length and the complex stability.[11–18] The basicity is therefore used as a measure of donor strength of the aromatic N-donors. The basicity of pyridine is mostly effected by inductive (I) or mesomeric (M) effects. Electronegative substituents cause a lowering of the basicity, due to −I-effect, while alkyl substituents (+I-effect) increase the electron density in the pyridine ring and consequently the basicity. Nevertheless, alkyl donor groups play a minor role compared to mesomeric effects caused by lone pairs conjugated to the pyridine nitrogen atom. Substituents with lone pairs have the strongest influence if they are located in ortho or *para* position, respectively. The Hammett constant σ is often used to quantify the electron donating or withdrawing ability of a certain substituent and correlates with pyridine basicity, which can be quantified by the pK_a value of the protonated form.[19–21] Figure 3 shows pyridine derivatives used in this study together with their Hammett constant and pK_a values from literature data.

It has been shown that Hammett constants of *para*-substituents in pyridine-based ligands correlate to electrochemical data of corresponding metal complexes. *Para*-substituted pyridines with increased basicity are used as ligands or as part of a more complex ligand structure in catalytically active metal complexes.[25–34] Depending on the catalysed reaction the increased donor ability of the pyridine can have a significant influence on the catalytic behaviour of these complexes and in some cases catalytic activity is increased.[25–26,31,34]

The effect of the basicity of aromatic N-donors on the catalytic behaviour of corresponding chromium polymerisation catalysts has not yet been investigated systematically. To the best of our knowledge very electron rich donor ligands like

[a] H.-B. Hansen, Prof. Dr. H. Wadepohl, Prof. Dr. M. Enders
Institute of Inorganic Chemistry
Heidelberg University
Im Neuenheimer Feld 270, 69120 Heidelberg, Germany
E-mail: markus.enders@uni-heidelberg.de

Supporting information for this article is available on the WWW under https://doi.org/10.1002/chem.202101586

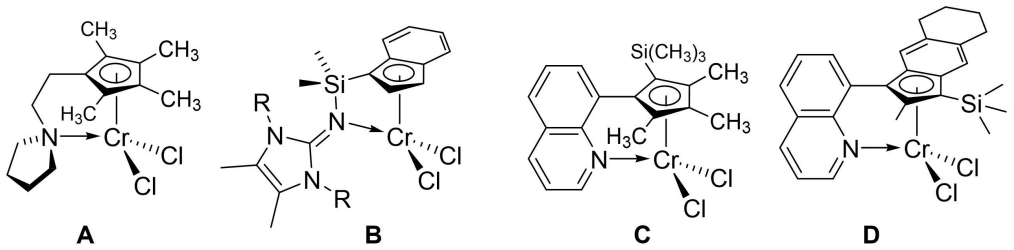

Figure 1. Examples of chromium pre-catalysts with N-donor functionalized cyclopentadienyl ligands.

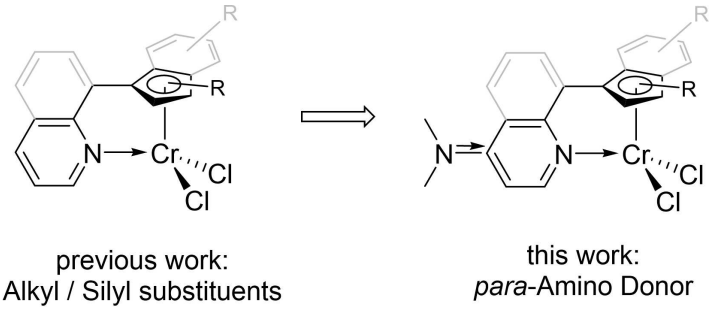

Figure 2. Previous and actual work on the influence of substituents.

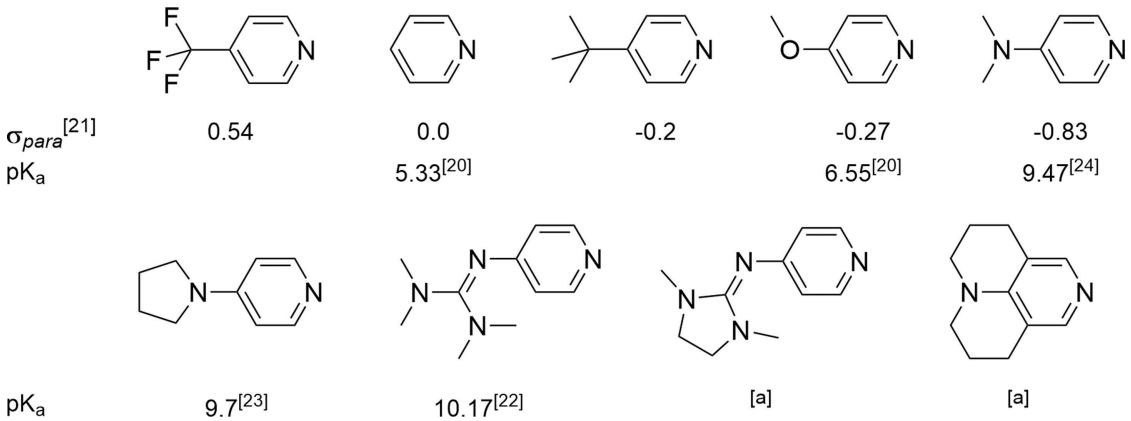

Figure 3. Pyridine derivatives used for ligand synthesis together with Hammett constants and reported pK_a values of the corresponding acids. The donor strength increases from left to right.[20–24] [a]: To the best of our knowledge no experimental pK_a value is available in literature.

dimethylaminopyridine (DMAP) have been used in olefin polymerization catalysts in only one example, a hafnium based catalyst described in a recent patent.[35] The starting point for the work presented here are chromium based pre-catalysts like compounds **C** and **D** (Figure 1) which already show an excellent polymerization behaviour for the production of UHMW-PE. We present the synthesis of a series of new chelating ligands, which keep the so far successful ligand core (i.e. anionic C_5 ring, C_2 spacer and neutral, sp^2 N donor atom). However, the donor strength of the N donor was increased stepwise by introduction of electron rich substituents. The influence of the donor strength on structural and electronic properties of the pre-catalysts is evaluated.

Results

Synthesis of new ligands and complexes

A systematic modification of the donor strength of pyridines or quinolines is possible by introducing substituents at the 4-position of the heterocycle (*para* relative to N atom). By choosing the 4-position, the influence of the substituent is mainly of an electronic nature since the catalytic centre is in a distal position. Due to the fact, that 4-substituted pyridines are readily available and pyridines can be easily combined with indenes, we focused on pyridine functionalized indenyl ligands (Scheme 1). In addition to that, we synthesized quinolyl based indenyl ligands and quinolyl based cp-ligands as well.

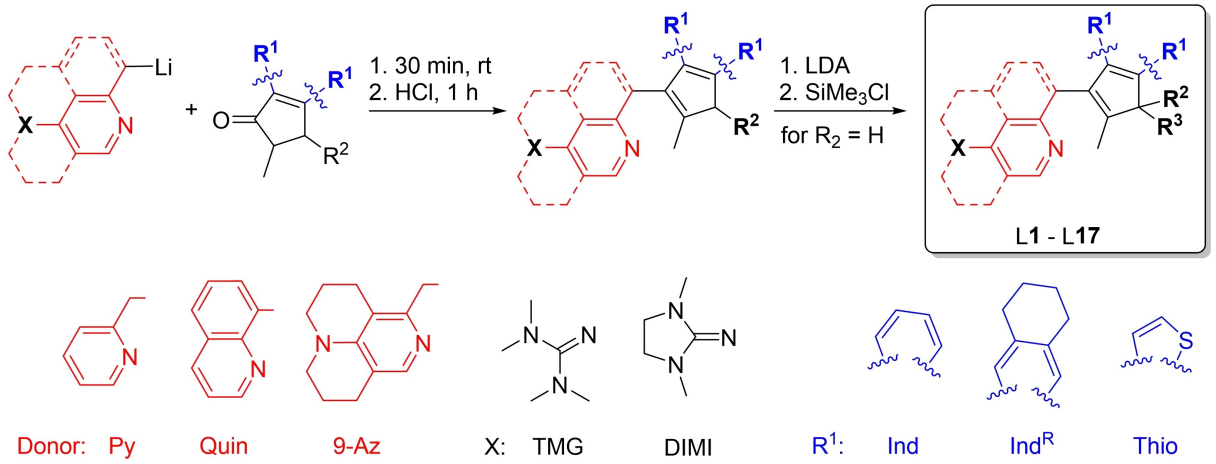

Scheme 1. Standard procedure for the synthesis of donor functionalized cp and indenyl ligands L**1**–L**17**. For synthetic details see Supporting Information.

The standard procedure to obtain suitable ligands is the lithiation of a 2-methyl-pyridine or an 8-bromoquinoline derivative with *n*-BuLi in situ and the subsequent reaction with an indanone or cyclopentenone. Water elimination from the resulting alcohol yields the corresponding protio-ligand, which can be further functionalized with a $SiMe_3$ group through subsequent deprotonation and addition of $SiMe_3Cl$ (Scheme 1). With this procedure we synthesized pyridine-based ligands L**1**–L**13** and quinoline based ligands L**14**–L**17** as summarized in Table 1.

In order to incorporate dimethylaniline as an electron-rich and bulky substituent on the indene or *cp* part, we used a different synthetic route: A cyclopentenone or an indanone derivative is reacted with N,N-dimethylanilline-4-magnesium-bromide leading to donor substituted cyclopentadiene or indene derivatives. Lithiation with *n*-BuLi and reaction with a suitable 2-(chloromethyl)pyridine gives the protio ligands L**18** and L**19**, respectively. (Scheme 2).

The protio ligands were deprotonated with either *n*-BuLi, KH or lithium diisopropylamide (LDA) to form the corresponding lithium salts in situ. It should be noted that deprotonation of silylated ligands L**1**–L**9**, and L**17** bearing an N-donor in the 4-position of the pyridine or quinoline, was only successful if LDA was used as a base. The use of *n*-BuLi and especially KH lead to partial cleavage of the Cp–Si bond in these cases. Salt metathesis with $CrCl_3(thf)_3$ gave the complexes **1**–**19** with yields from 30–80 % (Scheme 3).

Complex Characterization

The synthesized indenyl complexes have colours from green to turquoise while cp complexes appear turquoise and deep blue. Most of the complexes are soluble in dichloromethane, while they are less soluble in tetrahydrofurane or toluene. In general, the solubility increases, when several alkyl or silyl substituents are present. Complexes **1**–**6** show a better solubility than **10**–**13**, while the CF_3 substituent leads to an exceptional good solubility. However, there are a couple of exceptions to this trend as the complexes **8** and **13** are of an unexpected very

Table 1. Combination of different substituents leading to protio ligands L**1**–L**17**. TMG = tetramethylguanidine, DIMI = dimethylimidazolidine-imine.

L	Donor	X	R^1	R^2	R^3
L1	Py	CF_3	Ind	H	$SiMe_3$
L2	Py	H	Ind	H	$SiMe_3$
L3	Py	^{t}Bu	Ind	H	$SiMe_3$
L4	Py	OMe	Ind	H	$SiMe_3$
L5	Py	NMe_2	Ind	H	$SiMe_3$
L6	Py	DIMI	Ind	H	$SiMe_3$
L7	Py	H	Ind^R	H	$SiMe_3$
L8	Py	pyrrolidine	Ind^R	H	$SiMe_3$
L9	Py	pyrrolidine	Thio	H	$SiMe_3$
L10	Py	NMe_2	Ind	H	–
L11	Py	pyrrolidine	Ind	H	–
L12	Py	TMG	Ind	H	–
L13	9-Az	–	Ind	H	–
L14	Quin	pyrrolidine	Ind	H	–
L15	Quin	TMG	Ind	H	–
L16	Quin	pyrrolidine	CH_3	CH_3	–
L17	Quin	pyrrolidine	CH_3	H	$SiMe_3$

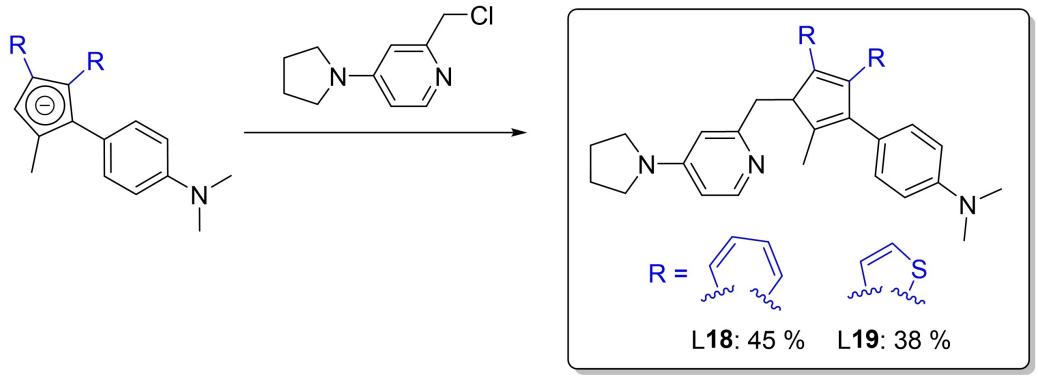

Scheme 2. Synthetic procedure for the ligands L**18** and L**19** with an N,N-dimethylaniline group.

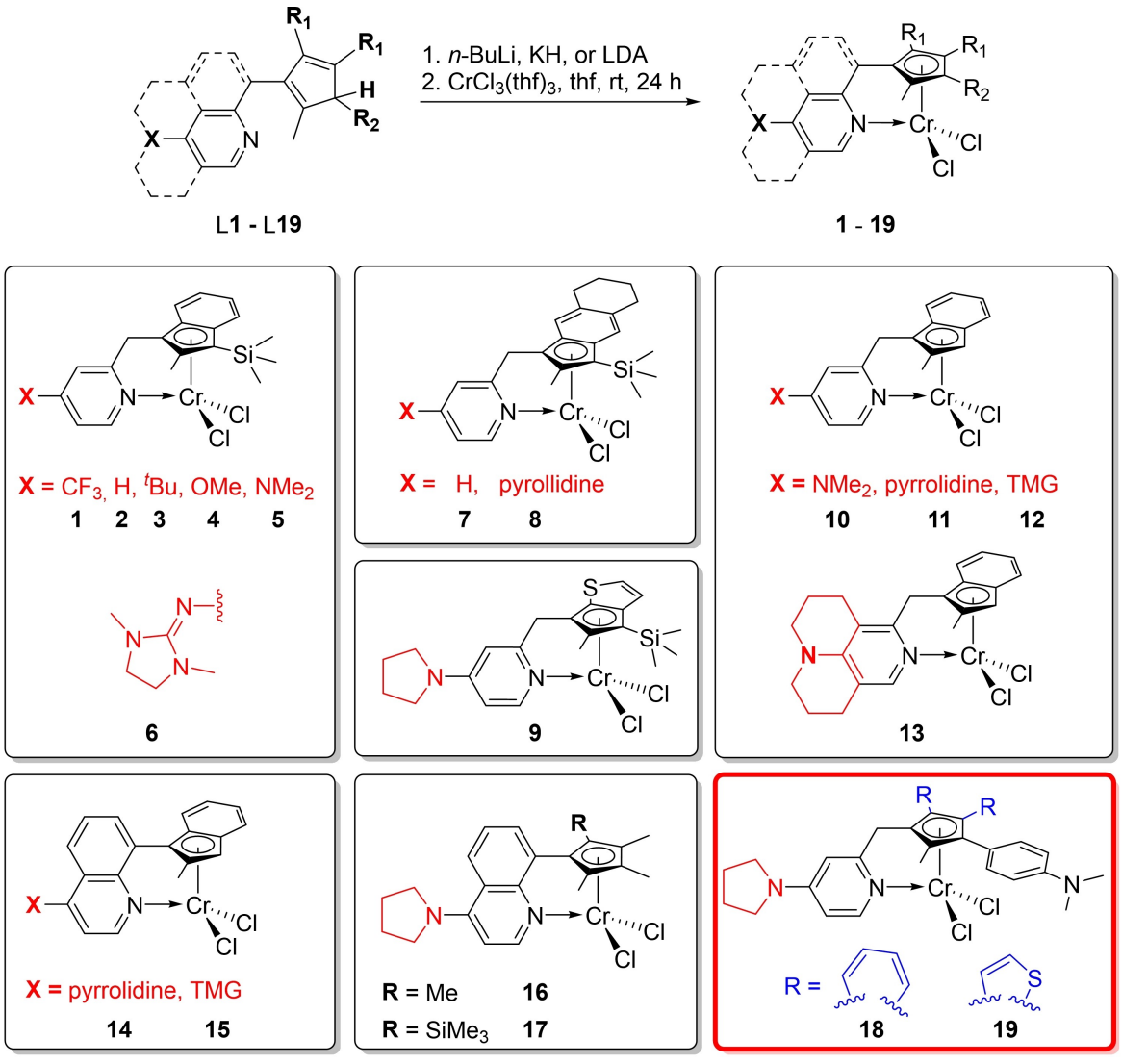

Scheme 3. Synthetic procedure and illustration of the new complexes **1**–**19**. The complexes are grouped by structural similarity. Complexes **18** and **19** showed the highest activity for indenyl and cp complexes of this type so far.

poor solubility. ^{1}H NMR spectra of the paramagnetic complexes are in accordance with the results of previous NMR investigation of chromium complexes of that type.[3] Single-crystal structure determination was successful for complexes **2**, **4**–**6**, **12**

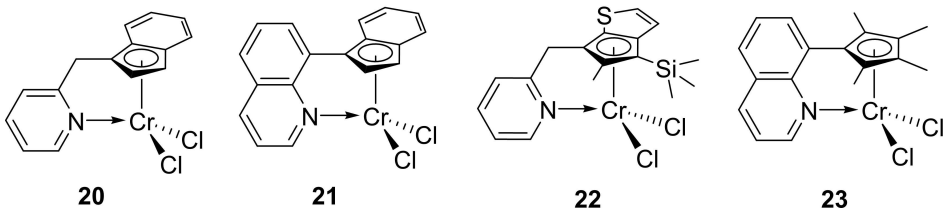

Figure 4. Literature known catalysts without 4-donor substituents used as reference.[2,36–37]

and **14**–**18** (Figures 5 and 6). X-ray quality crystals were generally obtained by slow diffusion of pentane into a dichloromethane solution. Complex **8** was crystalized by slowly cooling a saturated solution in chlorobenzene from 120 °C to room temperature.

A comparison of X-ray data of the new complexes and of previously published complexes **20**,[36] **21**,[2] **22**[37] and **23**,[2] (Figure 4) shows, that the Cr–N distance shortens when electron donating groups are installed at the 4 position of the aromatic donor. Complexes **1**–**6** can be directly compared with each other since they only differ in the 4-position of the pyridine. The experimental (**2**, **4**–**6**) and calculated (**1**-**6**) Cr–N bond lengths show a correlation with the Hammett constant of the corresponding substituent and the maximum of the electronic absorption spectra λ_{max} (see Table 2). Calculations were done by DFT modelling, using the uB3LYP functional and a 6-311G basis set. The calculated bond lengths in gaseous phase differ from the experimental values in the solid state but follow the same trend. The Cr–N distances of complexes **7** to **19** are shortened in the same way compared to similar complexes without a donating 4-substituent. Only the experimental Cr–N distances of **7** and **8** do not follow this trend (they are equivalent within experimental errors).

If the donor strength at the five membered ring is increased, the interaction with the metal atom is stronger so that the Cr–N distance becomes larger. This effect is visible by comparison of complexes **20** (Cr–N: 2.1076(11) Å, no substituents at the indenyl) with **2** (Cr–N: 2.1199(10) Å, $SiMe_3$ and CH_3 group at indenyl).

All complexes were characterized by UV-Vis absorption spectroscopy in dichloromethane solution. The wavelength of the absorption maximum in the visible region (λ_{max}) increases with the electron donating ability of the pyridine in complexes **1**–**6**. The absorption maximum shifts from 688 nm (**1**) to 702 nm (**6**), if substitution is changed from CF_3 to 1,3-diimethylimidazolidin-2-imine respectively (Table 2). A plot of UV-Vis spectra demonstrating this effect is presented in Figures S1.1 and S1.2 (see Supporting Information). The correlation of

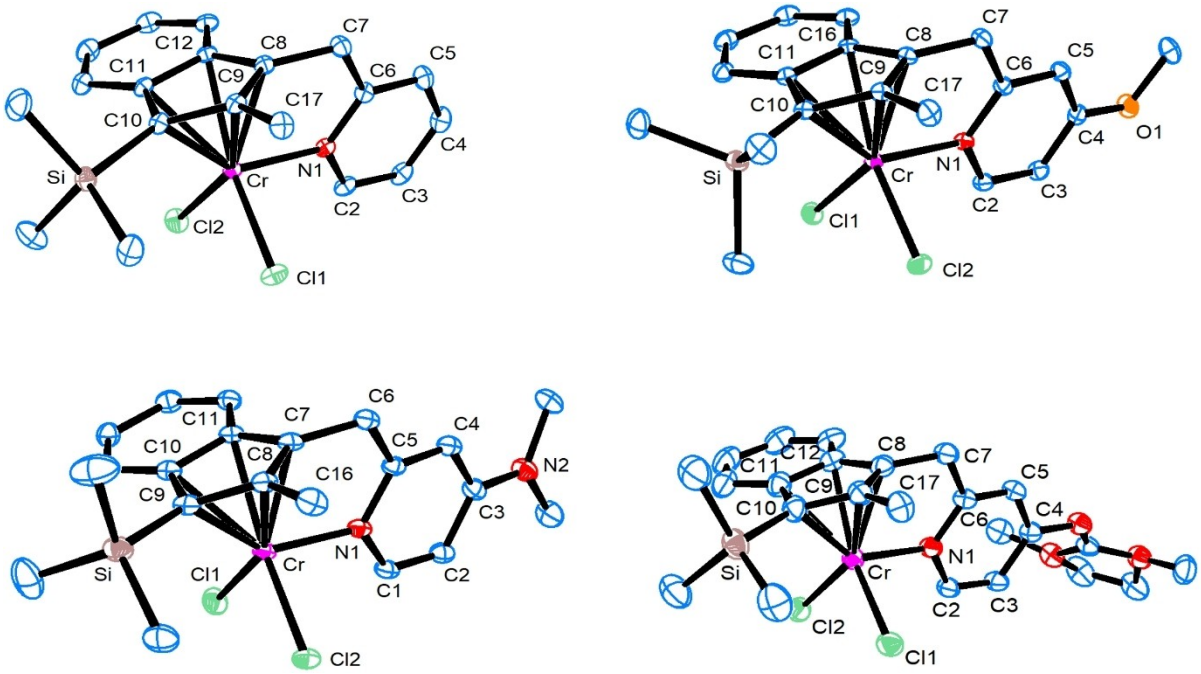

Figure 5. Molecular structures as obtained from x-ray diffraction of complexes **2**, **4**, (top) **5**, **6** (bottom, from left to right). Blue: C, red: N, green: Cl, purple: Cr, beige: Si, orange: O. H atoms and solvent molecules are omitted for clarity. Displacement ellipsoids are drawn with 50% probability. For details of crystal structure analysis see Supporting Information.

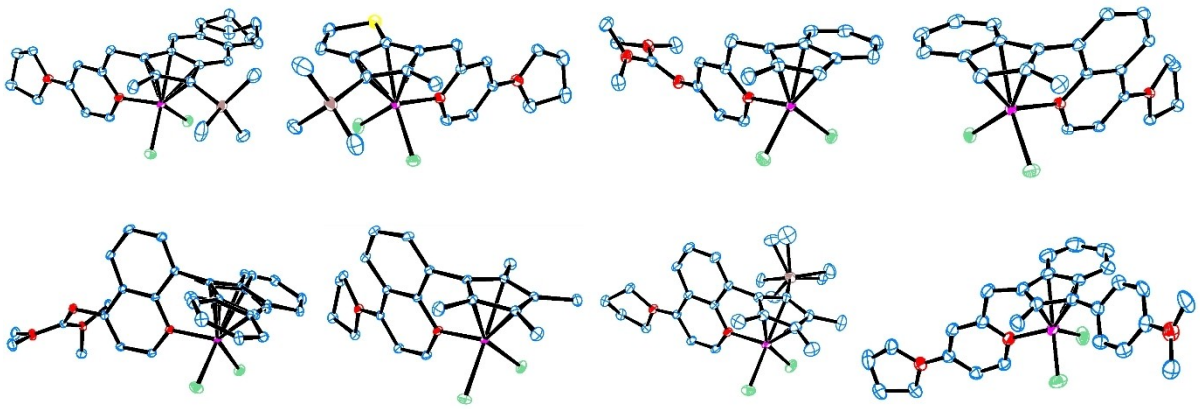

Figure 6. Molecular structures of complexes, **8**, **9**, **12**, **14** (upper line, from left to right) and **15**–**18** (lower line, from left to right). Blue: C, red: N, green: Cl, purple: Cr, brown: Si, yellow: S. H atoms and solvent molecules are omitted for clarity. Only one of two independent molecules is shown for complexes **17** and **18**. Displacement ellipsoids are drawn with 50% probability. For details of the crystal structure analysis see the Supporting Information.

Table 2. Experimental and calculated Cr–N bond lengths together with the Hammett constant σ_{para}, the pK_a values of the corresponding pyridine and the maximum of the electronic absorption spectra λ_{max}. Values in square brackets refer to a second independent molecule in the crystal. DIMI = dimethylimidazolidine-imine. [a]: No crystal could be obtained for **1** and **3**. [b]: No value was available from literature. For details see Supporting Information.

complex	indenyl substituent	4-substituent	Cr–N [Å] exp.	Cr–N [Å] calc	σ_p [21]	pK_a	λ_{max}
20	H, H	H	2.1076(11)	2.13234	0	5.33[20]	682
1	Me, SiMe3	CF3	–[a]	2.15123	0.54	-[b]	687
2	Me, SiMe3	H	2.1199(10)	2.13952	0	5.33[20]	689
3	Me, SiMe3	tBu	–[a]	2.12988	-0.2	-[b]	692
4	Me, SiMe3	OMe	2.1008(11)	2.12507	-0.27	6.55[20]	695
5	Me, SiMe3	NMe2	2.079(2)	2.10981	-0.83	9.47[24]	701
6	Me, SiMe3	DIMI	2.076(2)	2.10489	–[b]	–[b]	702
18	Me, dimethylaniline	pyrrolidine	2.055(2) [2.067(2)]	2.11156	–[b]	9.70[23]	715

calculated Cr–N distance, σ and λ_{max} is presented in Figure 7. Even the catalytic activity of these complexes reflects this trend to some extent.

All other complexes (**7**-**19**) show a similar behaviour: An increased donor strength of the N-donor ligand leads to a shift of the absorption bands to lower energies (Table S1, Supporting Information) and the colour of the complexes shifts from green (**7**, **20**, **21**, **23**, **C**: no 4-substituent) to turquoise (**8**, **10**–**13**, **14**, **15**)or blue (**9**, **16**, **17**, 4-amino substituent). Complex **18** and **19** have a bright green colour due to some additional strong absorption band around 400 nm caused by the dimethylaniline substituent.

Changing the substituents at the *para*-amino group has practically no effect on the colour, λ_{max} and Cr–N bond length (e.g. **5** versus −6 and **10** versus **11**, **12** or **13**).

Not only the donor ability of the pyridine influences λ_{max} but also the donating ability of the five-membered ring: If a methyl and a $SiMe_3$ substituent (**2**) is present, λ_{max} increases from 682 nm (no substituents, **20**) to 689 nm (**2**, Table 2). The strong electron donating dimethylaniline substituent has an even larger effect, as it shifts λ_{max} from 702 nm (**6**) to 715 nm (**18**, Table 2).

This demonstrates that the electron donating ability of both, the N-donor and the five-membered ring is able to alter the energies of the frontier molecular orbitals in a regular, almost additive manner. With these findings in mind, we then evaluated the influence of the ligand donor strength to the olefin polymerization behaviour of the resulting single-site chromium catalysts.

Ethylene homo and copolymerization

The new complexes were tested in ethylene homopolymerization and ethylene/1-hexene copolymerization experiments. In order to compare the catalytic behaviour as a function of the ligand structure we, used standardized conditions (see description of Tables 3 and 4). We focused on the influence of the electron donating groups and therefore used corresponding complexes without additional para N-donor (**7**, **22**) and the catalysts described above such as **C**, **20**, **21** and **23** as references. We only performed experiments with catalysts supported on SiO_2 with a view to the potential use of the new complexes in multicomponent systems.[6,8] The pre-catalysts were activated with MAO and supported with the incipient wetness method.[38] The polyethylenes (PE) obtained were characterized with differential scanning calorimetry (DSC), viscositmetry and ^1H NMR spectroscopy (for the co polymers). The molecular weight was determined from the intrinsic

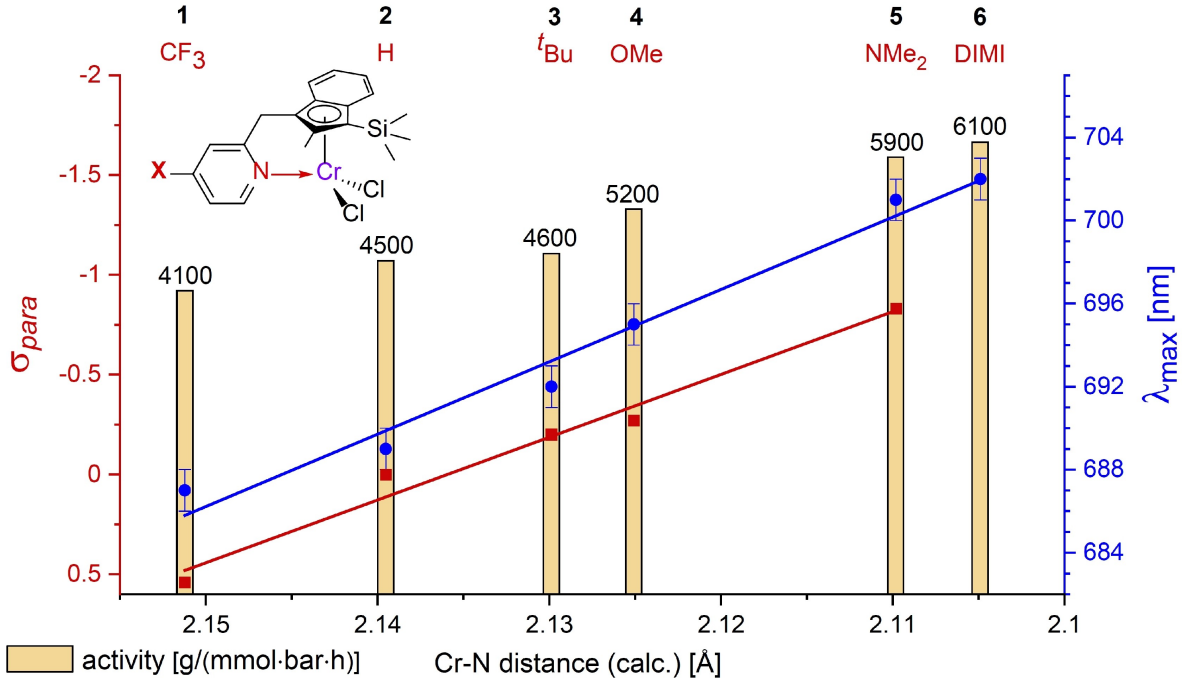

Figure 7. Plot of the calculated Cr–N distance vs. Hammett constant σ and the maximum of absorption spectra λ_{max} of complexes **1**, **2**, **3**, **4**, **5**, **6** (from left to right). Corresponding catalytic activities are given as coloured bars. No σ-value for **6** was available in literature. DIMI = dimethylimidazolidine-imine.

Table 3. Results of ethylene homopolymerization experiments.

exp. #	complex	activity[a]	mass [g]	IV[b] [dL/g]	Mv[c]	ΔH_m [J/g]	T_m [°C]	crist.[d] [%]
1	**20**	2700	2.7	9.25	917 276	124	134	42.9
2	**10**	5100	5.1	17.1	2 214 000	151	138	52.2
3	**11**	5500	5.5	15.4	1 895 000	132	137	45.7
4	**12**	5200	5.2	18.7	2 507 000	143	135	49.5
5	**13**	4600	4.6	18.3	2 427 000	139	137	48.1
6	**1**	4100	4.1	13.6	1 588 000	136	137	47.1
7	**2**	4500	4.5	20.7	2 903 000	129	134	44.6
8	**3**	4600	4.6	18.6	2 496 000	142	135	49.1
9	**4**	5200	5.2	16.4	2 070 000	139	134	47.8
10	**5**	5900	5.9	12.6	1 422 000	135	137	46.7
11	**6**	6100	6.1	20.4	2 841 000	131	135	45.3
12	**7**	5200	5.2	14.9	1 806 000	134	136	46.4
13	**8**	6500	6.5	11.4	1 236 000	142	136	49.1
14	**22**	4000	4.0	9.83	1 001 000	146	137	50.5
15	**9**	5400	5.4	10.8	1 148 000	155	136	53.6
16	**21**	2700	2.7	15.3	1 888 000	112	136	38.9
17	**14**	5400	5.4	18.4	2 443 000	140	135	48.4
18	**15**	5700	5.7	24.0	3 590 000	127	135	43.9
19	**C**	3500	3.5	10.3	1 076 000	147	136	50.9
20	**16**	4100	4.1	12.3	1 383 000	156	137	54.0
21	**17**	4500	4.5	12.1	1 338 000	156	136	54.0
22	**18**	6900	6.9	20.8	2 911 000	139	135	48.1
23	**19**	6000	6.0	20.2	2 796 000	159	135	55.0

Reaction conditions: 40 °C, 1 bar ethylene pressure, 30 min, 100 mL *n*-heptane, solid support: SiO_2, 1 mmol Triisobutylaluminum, 2 µmol [Cr], 2 mmol MAO, a = g PE mmol^{-1} h^{-1} bar^{-1}, b: intrinsic viscosity, c: Mv calculated with Mark-Houwink equation from intrinsic viscosity with $K = 6.2 \cdot 10^{-4} \cdot$ dL g^{-1} α[41] = 0.7, d: crystallinity of PE.

viscosity. The 1-hexene content was measured with ^{1}H NMR spectroscopy.

For a better comparison of the catalytic behaviour, the complexes were grouped according to structural similarity. In this way it is possible to ascribe the observed effects to specific ligand structures. The results of the homo- and co-polymerization experiments are given in Tables 3 and 4.

Table 4. Results of ethylene/1-hexene copolymerization experiments

exp. #	complex	1-hexene [ml]	activity[a]	mass [g]	IV[b] [dL/g]	Mv[c]	CH_3/ 1000 C	1-hexene [wt %][d]	ΔH_m [J/g]	T_m [°C]	crist. [%][e]
24	**20**	2	2000	2.0	8.22	835 000	10.3	6.2	91.5	117	31.7
25	**10**	2	4400	4.4	2.68	156 000	15.2	9.1	72.6	110	25.1
26	**11**	2	4500	4.5	7.46	675 000	17.0	10	81.2	113	28.1
27	**12**	2	4300	4.3	8.24	778 000	17.6	11	69.7	112	24.1
28	**13**	2	3900	3.9	7.64	698 000	16.7	10	79.2	115	27.4
29	**1**	2	3500	3.5	9.81	997 000	12.0	7.2	60.2	117	20.8
30	**2**	2	3700	3.7	9.02	885 000	13.5	8.1	62.3	117	21.6
31	**3**	2	3500	3.5	8.10	758 000	12.8	7.7	63.2	115	21.9
32	**4**	2	4400	4.4	6.87	600 000	11.4	6.9	60.6	116	21.0
33	**5**	2	5400	5.4	7.06	624 000	14.5	8.7	76.9	114	26.6
34	**6**	2	5500	5.5	10.8	1143 000	12.8	7.7	81.3	117	28.1
35	**7**	2	4200	4.2	7.36	662 000	13.6	8.2	70.8	119	24.5
36	**8**	2	6000	6.0	4.65	343 000	14.0	8.4	114	121	39.7
37	**22**	2	4100	4.1	7.88	730 000	11.3	6.8	93.0	115	32.2
38	**9**	2	5200	5.2	4.33	310 000	13.2	8.0	97.5	117	33.7
39	**21**	2	2600	2.6	8.64	832 000	10.8	6.5	90.3	113	31.3
40	**14**	2	3400	3.4	7.69	705 000	14.7	8.8	69.5	113	24.1
41	**15**	2	3600	3.6	4.62	340 000	15.5	9.3	66.8	113	23.1
42	**C**	2	2500	2.5	6.92	606 000	10.7	6.4	91.8	119	31.8
43	**16**	2	4100	4.1	6.76	586 000	9.30	5.6	116	123	40.0
44	**17**	2	3000	3.0	6.62	569 000	6.75	4.1	104	123	36.1
45	**18**	2	7200	7.2	5.67	456 000	30.0	18	57.8	112	20.0
46	**18**	7.5	7600	7.6	3.33	213 000	63.3	38	5.55	107	1.92
47	**18**	20	6000	6.0	2.66	154 000	101	61	1.56	-	0.54
48	**19**	2	6600	6.6	6.77	587 000	22.0	13	72.3	114	25.0

Reaction conditions: 40 °C, 1 bar of ethylene, 30 min, 100 mL of *n*-heptane, 2 μmol [Cr], 2 mmol MAO, solid support: SiO_2, co-monomer: 1-hexene, 1 mmol Triisobutylaluminum, a = g PE $mmol^{-1}\ h^{-1}\ bar^{-1}$, b: intrinsic viscosity, c: Mv calculated with Mark-Houwink equation from intrinsic viscosity with $K = 6.2 \cdot 10^{-4} \cdot dL\,g^{-1}$ $\alpha^{[41]} = 0.7$, d: 1-hexene content determined by ^1H NMR spectroscopy of PE in tetrachloroethane at 120 °C, e: crystallinity of PE.

Homopolymerization results

All tested catalysts produced PE close to or in the UHMW range at ambient pressure. The results of hompolymerization experiments show, that the introduction of an additional donor in the 4-position of the pyridine or quinoline generally increases catalytic activity and leads to higher molecular weights. The Mv produced by reference catalyst **20** is just beneath 1 Mio. g/mol, while the catalytic activity is 2700 g/(mmol bar h). Similar catalysts with more electron rich ligand systems produce twice as long PE chains approximately. Depending on the donor and the overall ligand structure, this effect is more or less remarkable. If complexes **10**–**13** with an additional 4-amino group are compared with the unsubstituted reference **20**, the catalytic activity and the produced molecular weight doubles approximately (Table 3, exp. 1–5). The effect of the additional methyl group alone is expected to be rather small.[10] It should be noted that complex **13**, that has the most electron rich pyridine, produced less PE than its analogues. This may be due to the very poor solubility of the pre-catalyst which hampers the catalyst activation procedure. The additional $SiMe_3$ group is able to increase catalytic activity and molecular weight as well. This effect becomes apparent by comparison of **2** with **20** (Table 3, exp. 7).

A comparison of complexes **1**–**6**, where only the substituent at the pyridine part is different, shows that the ligand donor strength not only correlates with the Cr–N bond length and the light absorption maximum (λ_{max}) (see above) but also with catalytic activity. The electron withdrawing CF_3 group in complex **1** reduces the activity, while electron donating groups increase activity. Nitrogen donors have a greater impact on the activity than ^{t}Bu or OMe, which follows the same trend as the Cr–N bond length and donor strength of the pyridine (Table 2 and Figure 7).

The good correlation as presented in Figure 7 is surprising, as catalytic activity in olefin polymerization depends on many parameters. On the other hand, the electronic effects of the pyridine substituents are efficiently transmitted to the active catalyst centre without changing the steric environment in the first coordination sphere. Therefore, the dependence of catalyst activity on ligand donor strength should be decoupled from other effects. Interactions between the Lewis basic nitrogen atoms of the distal donors and Lewis acidic aluminium sites in MAO may also be a factor influencing the catalyst behaviour. However, we have no experimental evidence for such interactions in the active catalyst. We assume that aluminium alkyls preferably bind to the surface of the polar support material.

As previously reported sterically demanding and more electron rich indenyl ligands like in complex **D** can improve catalytic properties as well.[5] Therefore we combined this indenyl moiety with para-pyrrolidinylpyridine to obtain complex **8**, that showed a catalytic activity even further increased compared to its less substituted analogue **7** (Table 3, exp. 12, 13).

A similar change in activity by additional para-N-donors is observed for the other groups of catalysts like indenyl-quinolyl complexes (**21**, **14**, **15**), cp complexes (**C**, **16**, **17**) and thiophene fused cp complex **9** as well. The positive effects of donor

substituents at the pyridine and indenyl or cp moiety regarding the catalytic activity seem to be additive to some extent. In line with this observation, the highest activity was obtained when two electron donating dialkylamino groups were installed at the ligand: One at the pyridine and a second as a N,N-dimethylaniline substituent at the five membered ring (complexes **18**, **19**). The activity of **18** and **19** are among the highest for indenyl and cp-chromium complexes we observed so far. In addition, Mv produced by cp complex **19** is dramatically higher than that of the $SiMe_3$ derivative **9**. We attribute these positive effects to a combination of a good electron donating ability and the steric bulkiness of the aniline substituent. The rigid structure of the aniline group prevents coordination of the NMe_2 group to the metal centre. An additional explanation for the preferential catalytic behaviour of **18** and **19** may come from interactions between the distant NMe_2 group and the MAO counter ion, which may lead to a more naked active species, as MAO is kept away from the metal centre.[39–40]

Copolymerisation results

Copolymerization experiments were carried out under the same conditions as the homo polymerizations but with additional 1-hexene in the reaction vessel. For comparison of co-monomer incorporation ability of the catalysts, it is sufficient to use only small amounts of co-monomer. Therefore, we used 2 ml of 1-hexene per 100 ml of *n*-heptane as standard concentration. In general, the overall ligand effects on the catalytic activity are the same as for the homo polymerization experiments: Electron donating groups at the ligand structure give enhanced activities, especially 4-N-donors at the pyridine or quinoline and the $SiMe_3$ or N,N-dimethylaniline group at the indenyl or cp moiety. Nevertheless, the activity and molecular weights decrease when co-monomer is present. For catalysts **18** and **19** a strong comonomer effect[42] can be observed, which gives them the highest activities of all performed experiments (Table 4, exp. 45–48). In general, the molecular weight strongly depends on the amount of incorporated co-monomer.

The co-monomer incorporation behaviour is also affected by the ligand structure. The electron donating *para*-substituents are able to increase 1-hexene content in all cases except the cp-quinolyl complexes **16** and **17** (exp. 42–44). This effect is rather strong for complexes **10**–**13**, which incorporate 10% 1-hexene, while complexes **1**–**9**, **14** and **15** give a 1-hexene content of 7–9%. In addition to the highest activities the complexes **18** and **19** also gave the best co-monomer incorporation of 18% and 13% respectively (exp. 45 & 48). Experiments with complex **18** and increased co-monomer concentration gave polymers with 1-hexene content of up to 60% (exp. 46 & 47). The highest activity was observed when 7.5 ml of 1-hexene were used per 100 ml of *n*-heptane, while it decreased when 20 ml were used. The DSC measurements of the latter polymer (exp. 47) did not show any specific melting point, which indicates a high level of amorphousness.

In summary, we observed that a stronger overall electron donating ability of the ligand lead to improved polymerization properties. The catalytic activity is significantly increased when additional N-donor substituents are present at the 4-position of the aromatic N-donor, whereas an N,N-dimethylaniline substituent at the cp or indenyl moiety is able to increase activity and comonomer incorporation as well.

Conclusion

We systematically altered the donor strength of pyridines and quinolines in donor functionalized indenyl and cp ligands and synthesized the corresponding chromium complexes. The addition of electron donating substituents at the *para*-position with respect to the coordinating N-atom increases the donor strength of these ligands. This leads to shorter Cr–N distances, which itself show an almost linear correlation with the corresponding Hammett constant and the electronic absorption maximum.

The complexes were tested in ethylene homopolymerization and ethylene/1-hexene copolymerisation experiments after activation with MAO. Catalysts with *para*-amino groups showed significantly higher catalytic activities compared to their less substituted analogues. The molecular weight of the produced polymer chains is also increased in most cases and lies in the UHMWPE range. A dimethylaniline moiety at the five membered ring proved to be favourable in terms of activity and comonomer incorporation. Derivative **18** showed an activity in ethylene homopolymerization of 6.9 kg polymer per mmol of catalyst at atmospheric pressure. In addition to that, the dimethylaniline group increase the comonomer incorporation ability.

We demonstrated that the catalytic activity is dependent on the electron donating power of the entire chelating ligand system. The combination of electron rich indenyl or cp moieties and strong donating aromatic N-donors gave the highest catalytic activities of this class of catalysts so far.

Experimental Section

See the Supporting Information for experimental details.

Deposition numbers 2060759–2060772 contain the supplementary crystallographic data for this paper. These data are provided free of charge by the joint Cambridge Crystallographic Data Centre and Fachinformationszentrum Karlsruhe Access Structures service.

Acknowledgements

The authors thank LyondellBasell Polyolefine GmbH (Frankfurt, Germany), in particular Dr. Shahram Mihan and Dr. Heike Gregorius, for discussion and support in polymer characterization. We greatly acknowledge financial support from the Federal Ministry of Education and Science (BMBF) within the project CATEFF (03XP0054D). We thank the state of Baden-Württemberg through bwHPC and the German Research Foundation (DFG) through grant no INST 40/467-1 FUGG

(JUSTUS cluster). Open access funding enabled and organized by Projekt DEAL.

Conflict of Interest

The authors declare no conflict of interest.

Keywords: chromium, ligand effects, olefin polymerization, supported catalysts, UHMW-PE

[1] A. Döhringr, J. Göhre, P. W. Jolly, B. Kryger, J. Rust, G. P. J. Verhovnik, *Organometallics* **2000**, *19*, 388–402.
[2] M. Enders, P. Fernández, G. Ludwig, H. Pritzkow, *Organometallics* **2001**, *20*, 5005–5007.
[3] P. Fernández, H. Pritzkow, J. J. Carbó, P. Hofmann, M. Enders, *Organometallics* **2007**, *26*, 4402–4412.
[4] S. Randoll, P. G. Jones, M. Tamm, *Organometallics* **2008**, *27*, 3232–3239.
[5] H.-B. Hansen, H. Wadepohl, M. Enders, *Eur. J. Inorg. Chem.* **2021**, *2021*, 1278–1286.
[6] A. Kurek, S. Mark, M. Enders, M. O. Kristen, R. Mülhaupt, *Macromol. Rapid Commun.* **2010**, *31*, 1359–1363.
[7] A. Kurek, S. Mark, M. Enders, M. Stürzel, R. Mülhaupt, *J. Mol. Catal. A* **2014**, *383*, 53–57.
[8] M. Stürzel, A. G. Kurek, T. Hees, Y. Thomann, H. Blattmann, R. Mülhaupt, *Polymer* **2016**, *102*, 112–118.
[9] D. Hofmann, A. Kurek, R. Thomann, J. Schwabe, S. Mark, M. Enders, T. Hees, R. Mülhaupt, *Macromolecules* **2017**, *50*, 8129–8139.
[10] M. Ronellenfitsch, T. Gehrmann, H. Wadepohl, M. Enders, *Macromolecules* **2017**, *50*, 35–43.
[11] P. T. T. Wong, D. G. Brewer, *Can. J. Chem.* **1968**, *46*, 131–138.
[12] D. G. Brewer, P. T. T. Wong, M. C. Sears, *Can. J. Chem.* **1968**, *46*, 3137–3141.
[13] P. T. T. Wong, D. G. Brewer, *Can. J. Chem.* **1969**, *47*, 4589–4597.
[14] M. C. Sears, W. V. F. Brooks, D. G. Brewer, *Can. J. Chem.* **1970**, *48*, 3786–3789.
[15] M. M. Tong, D. G. Brewer, *Can. J. Chem.* **1971**, *49*, 102–104.
[16] J. C. Chottard, D. Mansuy, J. F. Bartoli, *J. Organomet. Chem.* **1974**, *65*, C19-C22.
[17] D. Sellmann, Shaban Y. Shaban, Frank W. Heinemann, *Eur. J. Inorg. Chem.* **2004**, *2004*, 4591–4601.
[18] F. Vögtle, A. Siebert, *Chem. Ber.* **1985**, *118*, 1556–1563.
[19] J. M. Darmon, Z. R. Turner, E. Lobkovsky, P. J. Chirik, *Organometallics* **2012**, *31*, 2275–2285.
[20] P. Comba, M. Morgen, H. Wadepohl, *Inorg. Chem.* **2013**, *52*, 6481–6501.
[21] C. Hansch, A. Leo, R. W. Taft, *Chem. Rev.* **1991**, *91*, 165–195.
[22] N. Foroughifar, K. T. Leffek, Y. G. Lee, *Can. J. Chem.* **1992**, *70*, 2856–2858.
[23] E. Rossini, R. R. Netz, E.-W. Knapp, *J. Chem. Theory Comput.* **2016**, *12*, 3360–3369.
[24] M. R. Chakrabarty, C. S. Handloser, M. W. Mosher, *J. Chem. Soc. Perkin Trans. 2* **1973**, 938–942.
[25] J. V. Obligacion, P. J. Chirik, *J. Am. Chem. Soc.* **2013**, *135*, 19107–19110.
[26] S. Kuriyama, K. Arashiba, K. Nakajima, H. Tanaka, N. Kamaru, K. Yoshizawa, Y. Nishibayashi, *J. Am. Chem. Soc.* **2014**, *136*, 9719–9731.
[27] K. Devaine-Pressing, L. N. Dawe, C. M. Kozak, *Polym. Chem.* **2015**, *6*, 6305–6315.
[28] V. A. Schmidt, J. M. Hoyt, G. W. Margulieux, P. J. Chirik, *J. Am. Chem. Soc.* **2015**, *137*, 7903–7914.
[29] N. A. Bumagin, *Catal. Commun.* **2016**, *79*, 17–20.
[30] S. Das, R. R. Rodrigues, R. W. Lamb, F. Qu, E. Reinheimer, C. M. Boudreaux, C. E. Webster, J. H. Delcamp, E. T. Papish, *Inorg. Chem.* **2019**, *58*, 8012–8020.
[31] T. P. Pabst, J. V. Obligacion, É. Rochette, I. Pappas, P. J. Chirik, *J. Am. Chem. Soc.* **2019**, *141*, 15378–15389.
[32] J. Corpas, P. Viereck, P. J. Chirik, *ACS Catal.* **2020**, *10*, 8640–8647.
[33] D. P. Lubov, O. Y. Lyakin, D. G. Samsonenko, T. V. Rybalova, E. P. Talsi, K. P. Bryliakov, *Dalton Trans.* **2020**, *49*, 11150–11156.
[34] F. Zhu, G. Yang, A. J. Zoll, E. V. Rybak-Akimova, X. Zhu, *Catalysts* **2020**, *10*, 285.
[35] D. Koenigs, D. D. Devore, B. C. Bailey, E. Szuromi, R. D. Grigg, D. M. Pwarson, N. T. McDougal, J. B. Etienne, S. Mukhopadhyay, WO 2020/132422A1 **2020**.
[36] S. Mihan, D. Lilge, P. de Lange, G. Schweier, M. Schneider, U. Rief, U. Handrich, J. Hack, M. Enders, G. Ludwig, *Monocyclopentadienyl complexes of chromium, molybdenum or tungsten.* US6838563 B2 **2005**.
[37] M. Ronellenfitsch, *Doctoral thesis thesis*, Heidelberg University (Heidelberg), **2016**.
[38] G. G. Hlatky, *Chem. Rev.* **2000**, *100*, 1347–1376.
[39] C. Müller, D. Lilge, M. O. Kristen, P. Jutzi, *Angew. Chem. Int. Ed.* **2000**, *39*, 789–792; *Angew. Chem.* **2000**, *112*, 800–803.
[40] S. K. Kim, H. K. Kim, M. H. Lee, S. W. Yoon, Y. Do, *Angew. Chem. Int. Ed.* **2006**, *45*, 6163–6166; *Angew. Chem.* **2006**, *118*, 6309–6312.
[41] W. Zeng, Y. Du, Y. Xue, H. L. Frisch, in *Physical Properties of Polymers Handbook* (Ed.: J. Mark), Springer New York, **2007**, pp. 305–318.
[42] M. P. McDaniel, E. D. Schwerdtfeger, M. D. Jensen, *J. Catal.* **2014**, *314*, 109–116.

Manuscript received: May 4, 2021
Accepted manuscript online: May 21, 2021
Version of record online: June 23, 2021

